PLOS ONE

RESEARCH ARTICLE

Genome-wide survey of the F-box/Kelch (FBK) members and molecular identification of a novel FBK gene *TaAFR* in wheat

Chunru Wei[1], Weiquan Zhao[2], Runqiao Fan[1], Yuyu Meng[1], Yiming Yang[1], Xiaodong Wang[2], Nora A. Foroud[3], Daqun Liu[2], Xiumei Yu[1,2]*

1 College of Life Sciences/Key Laboratory of Hebei Province for Plant Physiology and Molecular Pathology, Hebei Agricultural University, Baoding, Hebei, China, **2** Technological Innovation Centre for Biological Control of Crop Diseases and Insect Pests of Hebei Province, Hebei Agricultural University, Baoding, Hebei, China, **3** Lethbridge Research and Development Centre, Agriculture and Agri-Food Canada, Lethbridge, Alberta, Canada

* yuxiumei@hebau.edu.cn

Citation: Wei C, Zhao W, Fan R, Meng Y, Yang Y, Wang X, et al. (2021) Genome-wide survey of the F-box/Kelch (FBK) members and molecular identification of a novel FBK gene *TaAFR* in wheat. PLoS ONE 16(7): e0250479. https://doi.org/10.1371/journal.pone.0250479

Editor: Jian Zhang, China National Rice Research Institute, CHINA

Received: March 30, 2021

Accepted: July 1, 2021

Published: July 22, 2021

Data Availability Statement: All relevant data are within the manuscript and its Supporting Information files.

Funding: CW was supported by the Postgraduate Innovation Funding Project of Hebei Province (CXZZBS2021046). XY received supports from the Natural Science Foundation of Hebei Province (C2020204050) and Scientific and Technological Research Projects of Higher Education of Hebei Province (ZD2019086). XW was supported by Natural Science Foundation of Hebei Province

Abstract

F-box proteins play critical roles in plant responses to biotic/abiotic stresses. In the present study, a total of 68 wheat F-box/Kelch (*TaFBK*) genes, unevenly distributed across 21 chromosomes and encoding 74 proteins, were identified in EnsemblPlants. Protein sequences were compared with those of Arabidopsis and three cereal species by phylogenetic and domain analyses, where the wheat sequences were resolved into 6 clades. *In silico* analysis of a digital PCR dataset revealed that *TaFBKs* were expressed at multiple developmental stages and tissues, and in response to drought and/or heat stresses. The *TaFBK19* gene, a homolog of the *Attenuated Far-Red Response* (*AFR*) genes in other plant species, and hence named *TaAFR*, was selected for further analysis. Reverse-transcription quantitative real-time PCR (RT-qPCR) was carried out to determine tissue-specific, hormone and stress (abiotic/biotic) responsive expression patterns. Of interest, *TaAFR* was expressed most abundantly in the leaves, and its expression in response to leaf rust variants suggests a potential role in compatible *vs* incompatible rust responses. The protein was predicted to localize in cytosol, but it was shown experimentally to localize in both the cytosol and the nucleus of tobacco. A series of protein interaction studies, starting with a yeast-2-hybrid (Y2H) library screen (wheat leaf infected with incompatible leaf rust pathogens), led to the identification of three TaAFR interacting proteins. Skp1/ASK1-like protein (Skp1) was found to interact with the F-box domain of TaAFR, while ADP-ribosylation factor 2-like isoform X1 (ARL2) and phenylalanine ammonia-lyase (PAL) were shown to interact with its Kelch domain. The data presented herein provides a solid foundation from which the function and metabolic network of TaAFR and other wheat FBKs can be further explored.

Introduction

In eukaryotes, the ubiquitin/26S proteasome system (UPS) is responsible for the selective degradation of most intracellular proteins [1]. Together with Suppressor of kinetochore protein 1

(C2021204008) and Provincial Supporting Program of Hebei for the Returned Oversea Scholars (C20190180). All of the funders had no role in study design, data collection and analysis, decision to publish, or preparation of the manuscript.

Competing interests: The authors have declared that no competing interests exist.

(Skp1), Cullin 1 (CUL1) and Ring-Box 1 (RBX1), F-box proteins form a ubiquitin ligase complex, where it plays the critical role of recruiting substrates to the UPS [2]. F-box proteins carry one or more 40–50 residue F-box/F-box-like domains in their N-terminus that are in charge of binding to Skp1/Skp1-like proteins [3]. Meanwhile, one or more additional conserved domains involved in substrate specificity can be found downstream of the F-box/F-box-like domain(s), such as Kelch repeats, Leucine Rich Repeat (LRR) and WD40-repeats [4]. The F-box members form a large family of proteins in plants, and within this family, the Kelch subfamily is one of the largest groups. Furthermore, F-box/Kelch (FBK) proteins are almost found in plants. The Kelch domain, originally identified in *Drosophila* mutants consists of 44–56 residues [5], and one or more Kelch domain(s) can be found in an FBK protein.

The size of the FBK subfamily varies depending on the plant species. In 2009, Xu et al. reported the identification of 96 FBKs in Arabidopsis, along with 27 and 35 FBKs from rice and poplar, respectively [6]. Using this information, Schumann et al. went on to identify additional FBKs in numerous species, and found: 103, 68 and 36 FBKs from the dicot species, *Arabidopsis thaliana*, *Populus trichocarpa* and *Vitis vinifera*, respectively; 44 and 39 FBKs in the monocot species, *Sorghum bicolor* and *Oryza sativa*, respectively; and 71 and 46 FBKs in the non-seed embryophytes *Physcomitrella patens* and *Selaginella moellendorffii*, respectively [7]. The former study reported that members of the FBK subfamily altered their protein structures by increasing or decreasing the number of exons, and the subfamily size was expanded primarily *via* tandem duplications [6]. The FBKs have been found to participate in biological clock regulation, photomorphogenesis, phenylpropanoid and pigmentation biosynthesis, and biotic stress responses [6,8–12]. While the FBKs subfamily exists in plants in relatively high numbers, and participates in many important biological processes, no systematic studies of the FBK subfamily have previously been reported in hexaploid wheat species.

To initiate FBK research in hexaploid wheat and to further our understanding of their role in various biological processes, a genome-wide identification study of this subfamily of F-box proteins is presented herein with a systematic analysis of protein structure, phylogenetic relationship, chromosome distribution, and expression patterns in response to different stresses. Sixty-eight genes encoding 74 wheat FBK (TaFBK) proteins were identified. *In silico* expression analysis for 47 of these genes revealed that they differentially regulated in response to drought and heat stresses. One gene, *TaFBK19*, which shows similarities to the *Attenuated Far-Red Response* (*AFR*) gene, was selected for further investigations, and is described here as *TaAFR*.

AFR F-box genes are involved in light signaling but have also been shown to participate in plant stress responses. Through the course of its cultivation, wheat is subjected to many kinds of environmental and biotic stresses including salt, drought, cold, heavy metals and various pathogens. These stresses can affect crop productivity and yield, which can be mitigated if a timely and appropriate stress response is mounted in the plant. To determine whether *TaAFR* is involved in the plant's response to different stress stimuli, the wheat line, TcLr15, was exposed to leaf rust pathogens, salt, drought and H_2O_2, salicylic acid (SA), abscisic acid (ABA) and methyl-jasmonate (MeJA), and changes in gene expression were assessed by reverse-transcription quantitative real-time PCR (RT-qPCR). Subcellular localization of TaAFR was experimentally determined, and its interactions with other proteins was investigated using a combination of yeast-2-hybrid (Y2H), bimolecular fluorescence complementation (BiFC) and co-immunoprecipitation (Co-IP) assays. While providing a glimpse into the function of TaAFR and other FBKs in wheat, the results presented herein build the foundation to further dissect the function and metabolic network of this important gene family.

Materials and methods

Genome-wide survey of wheat FBKs

Database search, sequence analysis and classification of wheat FBKs. The Hidden Markov Model (HMM) profiles of the F-box domain (PF00646, PF15966), F-box-like domain (PF12937, PF13013) and Kelch domain (PF01344, PF07646, PF13415, PF13418, PF13854, PF13964) were obtained from Pfam (http://pfam.xfam.org/). To identify wheat FBKs, the HMMER3.1b2 software was first used to search for F-box and F-box-like domains encoded in wheat genes deposited in the IWGSC (Wheat Genome Sequencing Consortium; RefSeq v1.0 wheat database downloaded from EnsemblPlants; https://plants.ensembl.org/index.html) (E value cut-off of 1.0) [13], and TBtools (v0.6673) was used to extract the target sequences. Sequences encoding F-box and F-box-like domains were further screened for the presence of one or more Kelch domains (E value cut-off of 1.0). Finally, Pfam, SMART (http://smart.-heidelberg.de/) and HMMER (web version 2.25.0, https://www.ebi.ac.uk/Tools/hmmer/) were adopted to confirm the presence of both the F-box (or F-box-like) and Kelch domains in each FBK protein identified, E value <1.0; sequences that did not meet this criterion were removed.

The predicted isoelectric point (*p*I) and molecular weight (MW) of the TaFBKs were computed using the Expasy Compute pI/Mw tool (https://web.expasy.org/compute_pi/). The intron-exon organization of wheat FBKs was obtained from EnsemblPlants. Subcellular localizations were predicted using the cropPAL2020 dataset (https://crop-pal.org/).

Analysis of conserved residues within the F-box and Kelch domains of wheat FBK proteins. The ClustalX2.0 multiple sequence alignment tool was used to align the F-box or Kelch domains extracted from the TaFBK protein sequences, and WebLogos (http://weblogo.berkeley.edu/) were generated for each of the two domains.

Phylogenetic analysis. In order to study the phylogenetic relationship and evolution of wheat FBKs, the obtained TaFBK sequences were compared with the orthologues from the model dicot species Arabidopsis (AtFBK), and three important monocots, namely rice (OsFBK), sorghum (SbFBK) and maize (ZmFBK). The AtFBK, OsFBK, SbFBK sequences reported by Schumann et al. and ZmFBKs reported by Jia et al. were downloaded and screened for the presence of the F-box and Kelch domains [7,14]. Sequences that did not carry both F-box and Kelch domain(s) were removed, leaving a total of 94, 31, 34 and 32 FBK protein sequences from Arabidopsis, rice, sorghum and maize, respectively. The FBKs from these four species were aligned together with the wheat FBKs using the ClustalX 2.0 algorithm and a phylogenetic tree was constructed by the Maximum Likelihood (ML) algorithm in MEGA7 using default parameters, with bootstrap value set to 1000 repetitions.

Chromosomal distribution and gene duplication analysis. The chromosomal distribution of wheat *FBK* genes was obtained from the EnsemblPlants (IWGSC RefSeq v1.0). MapDraw was used to visualize the detailed location of each *TaFBK* gene on the wheat chromosome [15]. Greater than 70% sequence similarity was set as the criterion for determining gene duplication [16]. When the maximum distance between duplicated genes on the same chromosome was smaller than 50 kb, tandem duplication and duplicated genes on different chromosomes were delimited as segmental duplications [17].

***In silico* expression analysis of *TaFBK* genes.** *FBK* gene sequences obtained from EnsemblPlants were input into the WheatExp wheat database (https://wheat.pw.usda.gov/WheatExp/) to identify the corresponding WheatExp gene ID. Using the zero to one normalized scale method, heat maps were constructed for the *TaFBK* genes collected from different digital PCR transcriptomics datasets in WheatExp. FPKM (Fragments Per Kilobase per million Mapped reads) values were obtained for the FBKs from 5 tissues (cultivar Chinese Spring) at different development stages: leaves (z10, z23, z71), roots (z10, z13, z39), stems (z30, z32, z65),

spikes (z32, z39, z65) and grains (z71, z75, z85) [18]. FPKM values were also downloaded from the wheat cultivar TAM 107 where leaves were treated with drought (DS), heat (HS) and drought+heat (HD) stresses [19]. TBtools (v0.6673) was used to draw a heat map according to their corresponding FPKM values.

Molecular identification and expression patterns of *TaAFR*

The wheat FBK gene, *TaFBK19*, was selected for further analysis. This gene is similar to the Kelch containing F-box *AFR* genes from other species and is therefore described here as *TaAFR*.

Plant material, fungal strains and inoculum preparation. A leaf rust resistant near-isogenic wheat line of Thatcher, TcLr15, and leaf rust strains 05-5-137③ and 05-19-43② were used in the present study. Unless otherwise specified, plants were grown in a greenhouse as described in Yu et al. [20]. Urediniospore and inoculum preparation of leaf rust pathogens were carried out as previously described [20].

***TaAFR* cloning.** Total RNA extraction and first strand cDNA synthesis were performed as previously described [20]. A pair of gene specific primers *TaAFR*-F and *TaAFR*-R (S1 Table) and Tks Gflex™ DNA Polymerase (TaKaRa, Japan) were used to amplify the full-length coding sequences (CDS) according to manufacturer's directions, with an annealing temperature of 56.4˚C. The purity of the amplicon was verified by 1.2% agarose gel electrophoresis and the product was sequenced to confirm the identity of the clone.

The TaAFR sequence was used to pull out related sequences from the NCBI transcript database using the BLASTp tool, and sequences with an expect threshold of <0.05 were aligned together with TaAFR in MEGA 7.0 and a phylogenetic tree was constructed, as described in the section on phylogenetic analysis. The TaAFR protein sequence was also analyzed using various bioinformatics tools to predict presence of signal peptides (SignalP-4.1, www.cbs.dtu.dk/services/SignalP/), transmembrane domains (TMHMM Server v. 2.0, www.cbs.dtu.dk/services/TMHMM/), and subcellular localization (cropPAL2020 dataset). The 3D structure was predicted in Phyre2 (www.sbg.bio.ic.ac.uk/phyre2/).

Wheat treatments and sampling for RT-qPCR. Sampling of wheat for gene expression analysis was carried out in different tissues (for tissue-specific analysis) and in response to three different types of abiotic stresses and three hormone treatments, as described below. For each experiment, samples were collected from three replicates and, unless otherwise specified, 3–5 samples were harvested for each replicate. Samples were flash frozen in liquid nitrogen and stored at −80˚C prior to RNA extraction.

To detect tissue-specific expression levels of the *TaAFR* gene, samples were collected from TcLr15 7-day old seedlings and adult plants grown in a pot with nutrient soil (Hebei Fengyuan, China) in a greenhouse (22˚C, 16 h light/8 h dark). Roots, stems and leaves were collected at z11; pistils, stamens and flag leaves were collected at z51. A large number of pistils and stamens (50–100 mg) were sampled from wheat florets.

To assess the effect of leaf rust pathogens on *TaAFR* expression, TcLr15 plants were inoculated with rust strains 05-5-137③ or 05-19-43②, or mock-inoculated with water, as previously described [20]. The inoculated and mock-inoculated leaves were harvested at 0, 6, 12, 24, 48 and 96 hours post inoculation (hpi). Mock-inoculated samples served as a negative control for each harvest time.

The effect of abiotic stress treatments on *TaAFR* expression was evaluated in TcLr15 plants grown in Hoagland's solution [21]. Once plants reached the three-leaf stage (z13), Hoagland's solution was amended with NaCl, PEG 6000 and H_2O_2, to a final concentration of 300 mM, 10% and 7 mM, respectively [22–24]. The second leaves were sampled at 0, 0.5, 2, 6, 12, 24 and

48 h post-treatment. Samples were also collected at the same time points from untreated negative control plants in Hoagland's solution.

The plant hormones, SA, ABA and MeJA, are known to be involved in both abiotic and biotic stress responses [25,26]. To investigate the effects of 3 hormones on the expression of *TaAFR*, exogenous treatments of SA (2 mM), ABA (100 μM) and MeJA (100 μM), each dissolved in 0.1% absolute ethanol [22,26], were applied to TcLr15 seedlings (z11) grown in a pot with nutrient soil in the greenhouse. The negative control plants were sprayed with 0.1% absolute ethanol. The primary leaf of each plant from treated and control samples was collected at 0, 0.5, 2, 6, 12, 24 and 48 h post-treatment.

Gene expression analysis by RT-qPCR. Total RNA was extracted from the TcLr15 samples collected in the previous section for gene expression analysis, using Biozol reagent (Bio-Flux, Japan), according to manufacturer's instructions. To eliminate gDNA contamination, 2 μg of each RNA sample was treated with 1 μL gDNA Remover (TransGen, China). cDNA synthesis was carried out as described by Yu et al. [20]. qPCR was performed on a Bio-Rad CFX Connect™ real-time PCR system (Bio-Rad, America). cDNA was diluted 2-fold (800 ng/μL), and 1 μL was used as the template in 20 μL qPCR reactions, with TransStart Top Green qPCR Super Mix (TransGen, China) and gene specific primers RT-qPCR-*TaAFR*-F and RT-qPCR-*TaAFR*-R (S1 Table), and the reaction carried out with an annealing temperature of 58.3˚C. A similar reaction was carried out using primers for the wheat reference gene *GAPDH* (GenBank: AF251217) (primers RT-qPCR-*GAPDH*-F and RT-qPCR-*GAPDH*-R, annealing temperature of 58.3˚C) (S1 Table). Three technical replicates were conducted for each of three biological replicates per sample. The relative expression of *TaAFR* was evaluated as described by Yu et al. [20]. For samples where a treatment was included, in order to take into account any potential changes in expression related to the circadian rhythm, the values of the control treatments collected at the specified harvest times were subtracted from those of the treated samples prior to comparing expression with the time zero untreated controls.

Subcellular localization. The *TaAFR* CDS, minus the stop codon, was inserted upstream of a GFP tag in the pSuper1300 vector (Laboratory preservation), and the recombinant construct was transformed into *Agrobacterium* GV3101. The strain GV3101-pSuper1300-*TaAFR* was injected into *N. benthamiana* leaves at the five-leaf stage, and then observed over a period of 30 to 80 h by fluorescence microscope (Nikon Ti 2, Japan) with an excitation wavelength of 495 nm.

Identification of TaAFR interacting proteins

Yeast-2-hybrid (Y2H). The *TaAFR* CDS was cloned into the yeast bait vector pGBKT7 which carries the GAL4 DNA-binding domain (BD), and the construct, BD-*TaAFR*, was subsequently transformed into yeast strain Y187. A yeast cDNA library (AD-*cDNA*) previously constructed was used to screen for partner proteins of TaAFR [27]. Y187-BD-*TaAFR* was co-cultured overnight in YPDA media with AH109-AD-*cDNA* at 30˚C with gentle agitation (50 r/min). The mated culture was spread onto Petri plates with SD-WLHA medium and incubated at 30˚C for 3–5 days. Positive clones were sequenced by Beijing Zhongke Xilin Biotechnology Co., Ltd., and the identity of the partner proteins were determined by BLAST alignments.

Once the identities of the positive interactions were determined, the CDS sequences were amplified from the cDNA of TcLr15 inoculated with leaf rust strain 05-19-43②. These coding sequences were then inserted into the pGADT7 (AD) vector to generate recombinant AD-*Prey* for re-testing the interactions with the bait protein in the BD-*TaAFR* construct. The interaction combination (TaTCTP and TaSnRK1) validated by Ma et al. was used as a positive

interaction control in Y2H interaction assay [28]. The strength of the positive Y2H interactions with BD-*TaAFR* can be further verified according to the blueness of the yeast colony by using the β-galactosidase in the SD-WLHA medium.

To determine which of the TaAFR domain(s) interact with the partner proteins, the cDNA sequences of each of the F-box (1–71 aa) and Kelch (72–383 aa) domains of *TaAFR* were inserted into BD vectors. AD-*Prey* that showed positive interactions with BD-*TaAFR* were then screened for interactions with each of these two domains (AD-*Prey* with BD-*TaAFR-F-box* or with BD-*TaAFR-Kelch*) using the Y2H assay as described above.

Bimolecular fluorescence complementation (BiFC). Y2H positive interactions were validated by BiFC. The CDS of *TaAFR* and the partner proteins were inserted into pSPY CE and pSPY NE vectors (Laboratory preservation) to construct the pSPY CE-*TaAFR* and pSPY NE-*Prey* vectors, respectively. GV3101 with pSPY CE-*TaAFR* and with pSPY NE-*Prey* were combined and co-injected into the *N. benthamiana* leaves. Fluorescence signal was observed as described in the subcellular localization section. The interaction combination (TaTCTP and TaSnRK1) was also used as a positive interaction control for the BiFC assay.

Co-immunoprecipitation (Co-IP). The positive interactions tested by BiFC were further validated by Co-IP. The CDS of *TaAFR* and the putative partner proteins were inserted into pTF101 (Laboratory preservation) with HA or FLAG tags to construct the recombinant vectors pTF101 HA-*TaAFR* and pTF101 FLAG-*Prey*, respectively. GV3101 strains with pTF101 HA-*TaAFR* and pTF101 FLAG-*Prey* were co-injected and transiently expressed in *N. benthamiana*. The combination of pTF101 HA-*TaAFR* and pTF101 FLAG-*TaGFP* was used as a negative control. Proteins were extracted from *N. benthamiana* leaves sampled 60 h after co-injection and subjected to IP by HA-magnetic beads, as described by Zhu and Huq [29]. The eluted proteins were subjected to immunoblot analysis with anti-FLAG tag polyclonal antibody (Solarbio, China).

Results

Genome-wide identification of wheat FBKs

74 Wheat FBK proteins were identified and divided into 5 categories based on their functional domains. The seed sequences of F-box (457), F-box-like (306) and Kelch (486) domains were obtained from the Pfam database. "F-box domain" will be used henceforth to describe both F-box and F-box-like domains. A total of 192 transcript sequences containing at least one F-box and Kelch domain were identified by searching the wheat IWGSC translated transcript database with HMMER3.1b2. Among these, 68 genes encoding 74 transcripts were found to carry both the F-box and Kelch domains, predicted by SMART and HMMER. The putative protein sequences (S1 File), *p*I, MW, number of introns, subcellular localization, and functional domains of the 74 putative wheat FBKs are presented in S2 Table. Wheat FBK (TaFBK) proteins range from 239 to 643 residues in length, with predicted MWs of 27.41–69.41 kDa and theoretical *p*Is of 4.18–9.99, of which the number of acidic/alkaline proteins account for half of the proteins, and 22 of these (29.7%) are greater than 9.0. Most of the TaFBKs were predicted to localize in the nucleus, cytoplasm or plastid, while a handful were predicted to localize in various organelles (peroxisome, golgi). The intron-exon structure has been reported to be closely related to the evolution of the F-box superfamily [30]. The number of introns identified in 74 *TaFBK* transcripts varies from 0 to 4, among them, 37 *TaFBK* transcripts are predicted to have 1 intron (50.0%) and 25 transcripts are predicted to have none (33.8%).

Each of the 74 *TaFBK* transcripts carry only one F-box domain at the N-terminus, with up to four Kelch domains at the C-terminus. A few members were also found to carry PAS and

PAC domains upstream of the F-box domain. According to their different domain structures, TaFBKs can be divided into 5 categories as follows: F-box+1 Kelch, F-box+2 Kelch, F-box+3 Kelch, PAS+F-box+4 Kelch, and PAS+PAC+F-box+4 Kelch (S1 Fig). The F-box+2 Kelch is the largest category, accounting for 40.5%, followed by F-box+1 Kelch (35.1%), while PAS +PAC+F-box+4 Kelch is the least represented with only 2 proteins in this group.

Wheat FBKs show conservation of F-box and divergence of Kelch domain sequences. MEGA7 was used to align the F-box or Kelch domains of TaFBKs. WebLogo's were generated, where the height of each stacked letter represents the probability that a given amino acid will occur at each position (S2 Fig). In the wheat F-box domain (S2A Fig), L-16 and R-18 are relatively tall, indicating a high probability that those residues would be found at those positions. In the F-box domain alignment, 69 and 65 of the 74 proteins analyzed, respectively carry L residues at the 16th position and R residues at the 18th position, which indicates that these 2 amino acids are conserved in the F-box domain of identified wheat FBKs. In addition, L-6 (82.4%), P-7 (81.1%), V-30 (87.8%) and W-34 (81.1%) were shown to be fairly conserved, followed by P-20 (73.0%), D-8 (68.9%), R-28(63.5%), R-32 (60.8%), D-9 (56.8%), C-31 (59.5%), V-19 (54.1%), C-15 (52.7%) and A-11 (51.4%).

The Weblogo of the Kelch domain (S2B Fig) shows that G-19 (85.8%), G-20 (86.4%), W-53 (97.9%) and M-59 (54.1%) are highly conserved. Although the height of some additional residues, such as R-2 (14.11%), H-5 (11.5%), L-10 (15.5%), G-12 (25.0%) and D-45 (20.3%), are relatively tall in the Kelch domain, according to the statistical assessment these are poorly conserved. Compared to the other protein sequences, TaFBK65 has 3 additional residues (PVP) at the N-terminus of the F-box motif; these 3 residues were removed from the analysis in order to prepare the Kelch WebLogo. In general, the amino acid sequences within the Kelch motif are more divergent than that observed within the F-box domain.

Phylogenetic grouping of the wheat, Arabidopsis, rice, sorghum and maize FBK subfamilies occurs according to the number of Kelch domains. To understand the evolutionary relationship of the 74 TaFBKs members, a phylogenetic tree was constructed using the protein sequences from 94 Arabidopsis FBKs (AtFBKs), 31 rice FBKs (OsFBKs), 34 sorghum FBKs (SbFBKs) and 32 maize FBKs (ZmFBKs) (Fig 1). The tree resolved into 7 clades, where the AtFBKs are mainly distributed in clade G, all of TaFBKs, OsFBKs, SbFBKs and ZmFBKs, with the exception of three OsFBKs (22, 14 and 9) and three SbFBKs (23, 16 and 8), distributed in clades A to F. All members in clade C belong to the F-box+1 Kelch type, and among them, only 5 members are from Arabidopsis, while the remaining 37 are from graminaceous species. In clades D and F, the FBKs of F-box+2 Kelch type account for the largest group, containing only a few members of F-box+1 Kelch and F-box+3 Kelch types. OsFBK31 and OsFBK28 (F-box+1 Kelch+RING) are also grouped into clade D. Clade E mainly consists of F-box+3 Kelch type FBKs from Gramineae and 3 members of F-box+2 Kelch proteins from Arabidopsis. FBKs with 4 Kelch domains (F-box+4 Kelch, PAS+F-box+4 Kelch, PAC+F-box+4 Kelch, and PAS+PAC+F-box+4 Kelch) are represented in 5 species and grouped in clade B. AtFBK54 (LSM14+F-box+2 Kelch) together with other members of Arabidopsis F-box+2 Kelch are in clade G. The phylogenetic analysis indicates that the number of Kelch domains is a key classification criterion within the FBK subfamily.

***TaFBK* genes are unevenly distributed on the wheat chromosomes and mainly expanded its size by segmental duplications.** The chromosomal position of 68 *TaFBK* genes were retrieved from EnsemblPlants and a chromosomal distribution map was generated (S3 Fig). The *TaFBK* genes are unevenly distributed on the wheat 21 chromosomes. The chromosomes of 4A (5), 4B (5), 6A (6), 6B (8), and 6D (6) have relatively higher distribution densities, whereas only one *TaFBK* gene was found on each of chromosomes 1B, 3B and 1D, and none were detected on chromosome 2B.

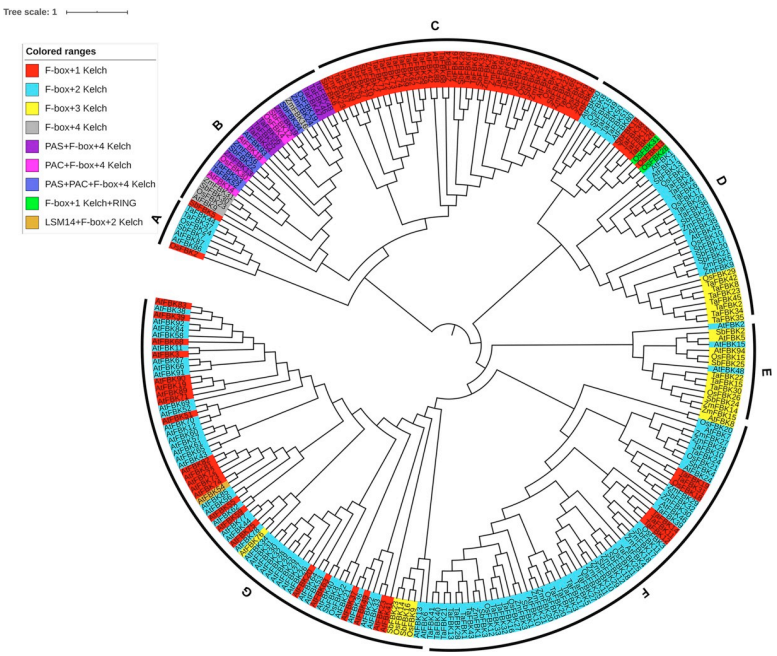

Fig 1. Phylogenetic analysis of FBK proteins in wheat, Arabidopsis and three important monocots. The full-length amino acid sequences were aligned by ClustalX 2.0 and the Maximum Likelihood (ML) tree was constructed using MEGA7. FBK proteins were grouped into 7 distinct clades named A-G.

https://doi.org/10.1371/journal.pone.0250479.g001

In animals, the number of F-box proteins is relatively low compared with plants, with only 68 and 74 F-box genes in the human and mouse genomes, respectively [31]. Incidentally, the wheat genome encodes the same number of the Kelch subfamily proteins, which represents only a portion of the F-box proteins encoded in this species. Gene duplication is thought to be the main driving factor in the expansion of the F-box family in plants [17]. To explore the evolutionary mechanism of the wheat FBK subfamily, the present study investigated tandem duplication and segmental duplication events in the wheat FBK subfamily of the F-box family by observing similarities among 68 FBK sequences. A total of 57 *TaFBKs* were identified to be segmental or, to a lesser extent, tandem duplications. Most of the segmental duplications, which are distributed on 20 chromosomes, included 1 or 2 duplication events (ie. 2 or 3 genes in the group), although as many as 7 segmental duplication events were observed. Tandemly duplicated genes affected 8 *TaFBK* genes, and each of these occurred on chromosome 4. These results indicate that both segmental and tandem duplications played a role in the expansion of the *TaFBK* subfamily, and unlike the results of Xu et al. in Arabidopsis and rice species [6], segmental duplications were more prolific in wheat.

Tissue-specific and abiotic stress response *in silico* expression of *TaFBKs*. To gleam insights into the putative functions of the identified wheat FBKs, *in silico* expression analysis of these genes was evaluated in different wheat tissues at different developmental stages, and in wheat leaves in response to environmental stresses. The FPKM values of *TaFBKs* from five different tissues and three stress combinations were downloaded from digital PCR data available in WheatExp (S3 Table) and were used to construct a heat map using the zero to one normalized scale method. Tissue-specific expression data (cultivar Chinese Spring) was available for 47 *TaFBKs* (Fig 2). In general, *TaFBK* genes exhibited differential expression in all five wheat tissues, suggesting that these genes may be involved in the developmental regulation of multiple tissues. There were two conditions where tissue-specific expression at specific

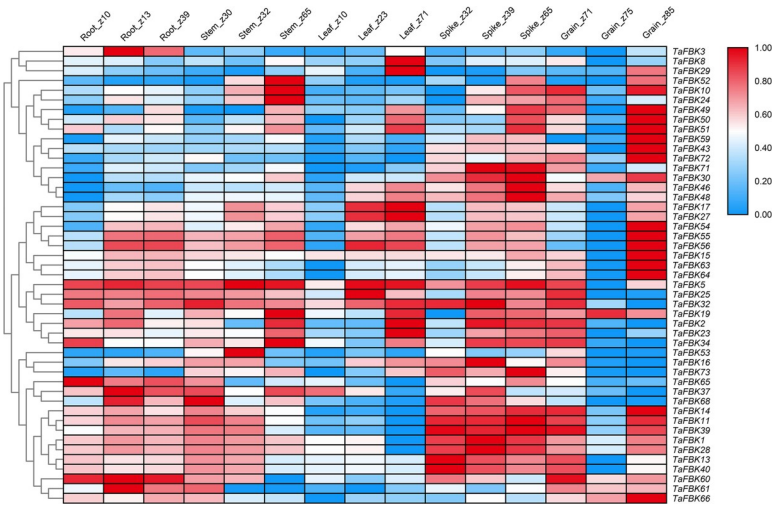

Fig 2. Heat map showing digital expression profiles of *FBK* genes in various tissues and at different developmental stages of wheat based on FPKM values. The color key represents FPKM values. Identity of tissue samples and developmental stages (Zadoks scale) are provided at the top of each lane.

https://doi.org/10.1371/journal.pone.0250479.g002

developmental stages showed significantly less transcript accumulation; these are leaf (z10) and grain (z75). Meanwhile, most *TaFBK* genes were generally more abundantly expressed in the spikes (z32, z39, z65) and grains (z71, z85). *TaFBK3* transcripts specifically accumulated in root tissues, *TaFBK8* and *TaFBK29* were dominantly expressed in mature leaf (z71), while *TaFBK60* and *TaFBK61* showed highest expression in root tissues followed by grain samples.

A second data set from the WheatExp database was analyzed for the effect of DS, HS and HD stresses on the expression of the same 47 *TaFBK* genes in seedlings of the wheat cultivar TAM 107. A heat map was generated for this dataset showing differential expression at 1 and 6 h (Fig 3). A general overview of expression of *TaFBK* genes affected by DS is as follows: 34.0% of the *TaFBK* genes were up-regulated; 47.0% of the genes showed strongly or slightly down-regulated expression; and 19.0% (9 transcripts) maintained stable expression between treatment and control. The following changes were observed in response to HS at 40˚C: transcripts *TaFBK60*, *TaFBK61* and *TaFBK*46 increased sharply at 1 h, and then decreased at 6 h; *TaFBK10*, *TaFBK23* and *TaFBK*50 expression gradually increased from 0 (control) to 6 h; eight *TaFBKs* were down-regulated at both time points assessed; the transcripts of seven genes (14.9%) decreased to roughly half of the control levels at 1 h; expression of the remaining 18 (38.3%) genes sharply declined at 1 h after the stress treatment, and transcript accumulation of 7 of these genes returned to levels similar to that of the control by 6 h, while the other 9 genes increased slightly at 6 h compared with the earlier time point. Following the combined treatment HD: 25.5% of the genes increased their expression from 1 to 6 h compared with the control; transcripts from 7 genes gradually decreased from 1 to 6 h; 72.3% transcripts sharply decreased at 1 h treatment, then slightly or sharply increased at 6 h. In brief, HS caused more obvious and intense change on expression of *TaFBKs* compared to the DS treatment.

Molecular identification and expression patterns of *TaAFR*

***TaAFR* gene encodes a wheat FBK protein.** The heat map presented in Fig 3 shows that the expression of *TaFBK19* was strongly up-regulated under DS treatment and sharply down-regulated under HS treatment at 1 h, while the HD treatment resulted in low level expression of this gene at both 1 and 6 h. *TaFBK19* was selected for further analysis. The full-length (1327

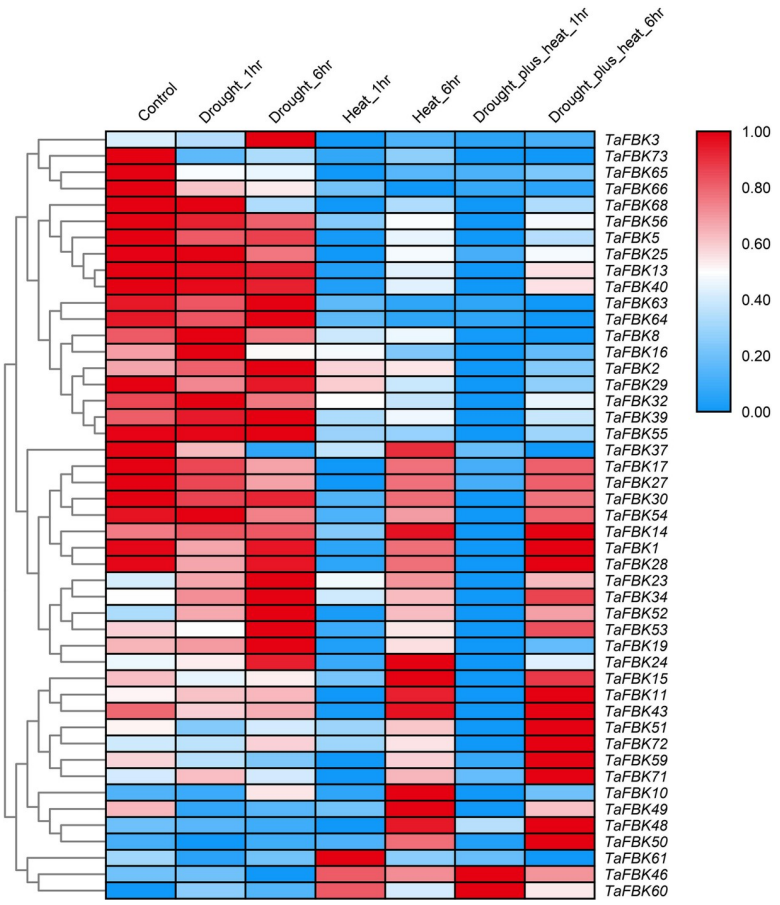

Fig 3. Heat map showing digital expression profiles of FBK genes in wheat response to DS, HS and HD based on FPKM values. FPKM values are represented by color according to the legend. The method and time of treatments are provided at the top of each lane. DS, drought stress; HS, heat stress; HD, heat+drought stresses.

https://doi.org/10.1371/journal.pone.0250479.g003

bp) cDNA sequence was cloned from TcLr15 wheat seedlings inoculated with the leaf rust strain 05-19-43②. The cDNA encodes a polypeptide with 383 amino acids. The predicted MW of the polypeptide is 40.69 kDa, and the predicted *p*I is 5.11. BLASTx analysis shows that the sequence shares high similarity (94%) with an F-box protein, AFR-like, from *Aegilops tauschii* (GenBank: XP 020194469.1). TaFBK19 protein carries a single highly conserved F-box domain (32–71 aa sites) at the N-terminus and a fairly divergent Kelch domain (136–174 aa sites) found in the internal region (Fig 4A). Phylogenetic analysis indicates that the TaFBK19 protein shares 94.10% and 87.47% similarity with AFR from *A*. *tauschii* and *Hordeum vulgare*, respectively, followed by AFR from *Brachypodium distachyon*, *O*. *sativa*, *Setaria italica*, *Panicum hallii*, *S*. *bicolor* and *Z*. *mays*. Meanwhile, AFRs from woody plants (*Prunus avium*, *Musa acuminata*, *Elaeis guineensis*, *Phoenix dactylifera*) and dicots (*Nelumbo nucifera*, *Dendrobium catenatum* and *A*. *thaliana*) were grouped in different clades (Fig 4C), which indicates that these FBKs are conserved in monocots. Based on the similarities between *TaFBK19* and *AFR* genes from other cereals and monocots, *TaFBK19* will henceforth be described as *TaAFR*. Sequence analysis of TaAFR did not reveal any predicted signal peptide or transmembrane domains, and the protein is predicted to localize to the cytosol. The predicted 3D structure shows three distinct α-helices at the N-terminus and β-sheets at the C-terminal end. The β-sheets are predicted to form 6 triangles, which further cluster to a regular hexagonal

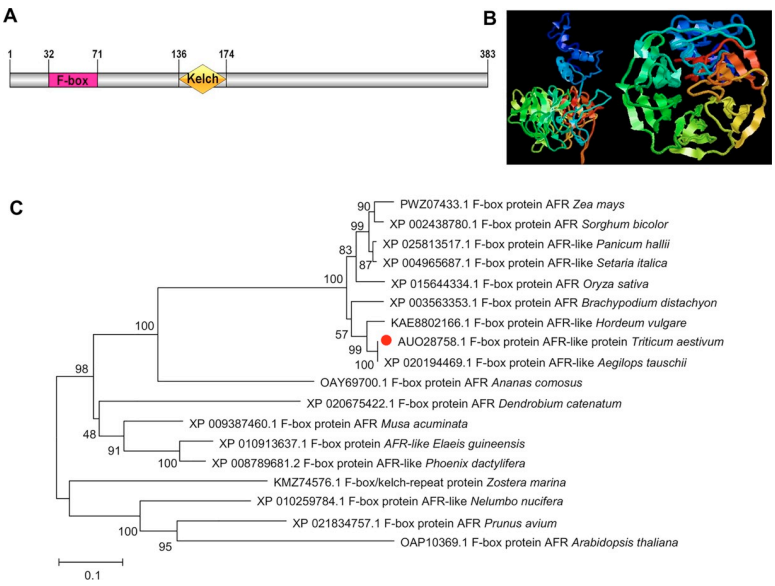

Fig 4. Sequence characteristics of wheat TaAFR. (A) Functional domain of TaAFR. A schematic diagram showing the positions of the F-box and Kelch domains in TaAFR; (B) 3D structure prediction of the TaAFR protein. The ribbons represent the α-helix structures, while the arrows denote the β-sheets. The colors highlight the position within the primary structure, with blue and red at the N- and the C-terminus, respectively; (C) Phylogenetic analysis of TaAFR with F-box proteins from different plants species. The phylogenetic tree was generated using the neighbour-joining method in MEGA 7. Branches are labeled with the GenBank accession number followed by species name.

https://doi.org/10.1371/journal.pone.0250479.g004

arrangement. These secondary and ultra-secondary structures indicate that the protein folds into chair-like configuration (Fig 4B).

***TaAFR* is primarily expressed in wheat leaves.** Six tissues were sampled from wheat seedlings (root, leaf and stem) and adult plants (pistil, stamen, flag leaf) of TcLr15 to analyze the tissue-specific expression of *TaAFR*. The young leaf was used as a control (the expression value was set 1.0) to measure its relative expression to other tissues. *TaAFR* was mainly expressed in young leaf, with lower expression in the flag leaf and extremely low expression was detected in young root, pistil, and stamen (Fig 5A).

Differential expression of *TaAFR* in incompatible and compatible wheat/leaf rust pathogen combinations. The temporal expression profile of *TaAFR* in TcLr15 leaves following inoculation with the two leaf rust strains, is shown in Fig 5B. Generally, the *TaAFR* transcript was higher in the compatible interaction (TcLr15 inoculated with 05-5-137③) than in the incompatible one (TcLr15 inoculated with 05-19-43②), except at 48 hpi. For the incompatible interaction, the *TaAFR* transcripts gradually increased from 6 to 96 hpi, but apart from the initial increase from 0 to 6 hpi, no significant difference was observed across the time course. In the compatible interaction, no significant change was observed between 0 to 48 hpi, but a rapid increase was observed at 96 hpi, where the expression of *TaAFR* transcripts was 3.1-fold higher than in the 0 h untreated control samples.

Expression of *TaAFR* is affected by salt, drought and oxidative stresses. Three abiotic stress treatments, salt (NaCl), drought (PEG 6000) and oxidative stress (H_2O_2), were evaluated for their effects on *TaAFR* expression in TcLr15 seedlings. The expression of *TaAFR* was significantly affected in TcLr15 after treatment with NaCl (Fig 5C). The transcripts were strongly up-regulated from 0.5 h, and maintained a high level of expression until 12 h. Two expression peaks occurred at 0.5 h (8.2-fold) and 6 h (7.9-fold). Thereafter, the *TaAFR* transcripts started to down-regulate gradually, until 48 h, where transcripts dropped to half of the level detected

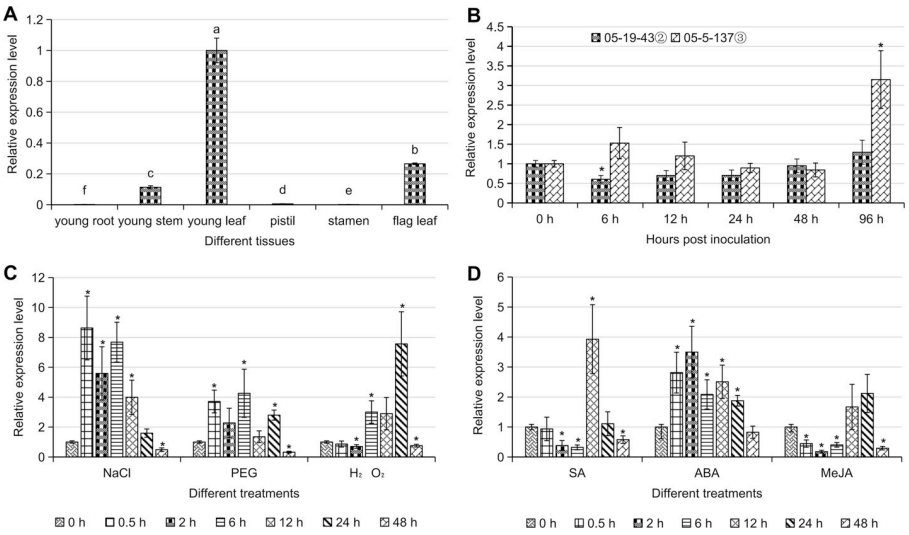

Fig 5. Expression patterns of *TaAFR* in different wheat tissues and in response to stresses/hormone treatments. (A) Expression profile of *TaAFR* in different tissues of TcLr15. Different letters indicate significant differences ($p < 0.05$). (B) Expression patterns of the *TaAFR* gene in incompatible and compatible combinations of TcLr15/*Puccinia triticina* strains 05-19-43② and 05-5-137③, respectively. (C) Effect of NaCl, PEG and H_2O_2 on *TaAFR* expression in TcLr15 leaves. (D) Effect of SA, ABA and MeJA on *TaAFR* expression in TcLr15 leaves. To remove the effect of the circadian cycle on *TaAFR* expression in B, C and D, the relative expression values for TcLr15 leaf control samples, harvested at the same time points as for the various treatments, was subtracted from the relative expression of the treatment samples at the specified harvest times. Relative expression, with the effect of the circadian cycle removed, was then compared to the 0 h untreated control; significant differences ($p < 0.05$) are marked with an asterisk.

https://doi.org/10.1371/journal.pone.0250479.g005

in the 0 h untreated controls. In response to PEG 6000 treatments, the *TaAFR* transcript was increased in abundance at 0.5 h (3.9-fold), 2 h (2.1-fold), 6 h (4.1-fold) and 24 h (3-fold), but was down-regulated at 48 h. After treatment with H_2O_2, the expression of *TaAFR* did not differ from that of the control until 2 h after treatment when it was down-regulated, but from 6 to 24 h, *TaAFR* showed an upward trend, reaching a peak at 24 h where it was 7.8-fold higher than that of the 0 h untreated control. Finally, expression levels dropped below that of the 0 h control at 48 h (Fig 5C).

Exogenous SA and ABA applications significantly up-regulate the expression of *TaAFR*. The expression pattern of *TaAFR* in TcLr15 following exogenous treatment with plant hormones is presented in Fig 5D. In response to SA treatments, *TaAFR* expression was down-regulated 2-fold at 2 and 6 h compared with the untreated 0 h control, and thereafter increased rapidly 4-fold at 12 h compared with the control before returning to the basal expression levels. In response to ABA, *TaAFR* expression increased rapidly by 3.5-fold, observed at 2 h, and continued to be up-regulated throughout the time course, but decreasing gradually until 48 h where basal level expression was observed. MeJA application resulted in significant down-regulation of *TaAFR* at most time points, except at 12 and 24 h, where no significant difference was observed compared with the control.

TaAFR is localized to the nucleus and cytoplasm. *N. benthamiana* was injected with GV3101 containing either the empty vector 35S:*GFP* or the recombinant vector 35S:*TaAFR-GFP*, and transient expression of the recombinant proteins was observed. The fluorescence signal of 35S:*GFP* was visualized in both the nucleus and cytoplasm 36 h after transfection (Fig 6), whereas the fluorescence signal of 35S:*TaAFR-GFP* was detected after 48 h, predominantly observed in the nucleus and cytoplasm. Moreover, the nuclear dye DAPI was used to stain the tobacco leaves after transfection, and a light blue color was clearly observed in the nucleus.

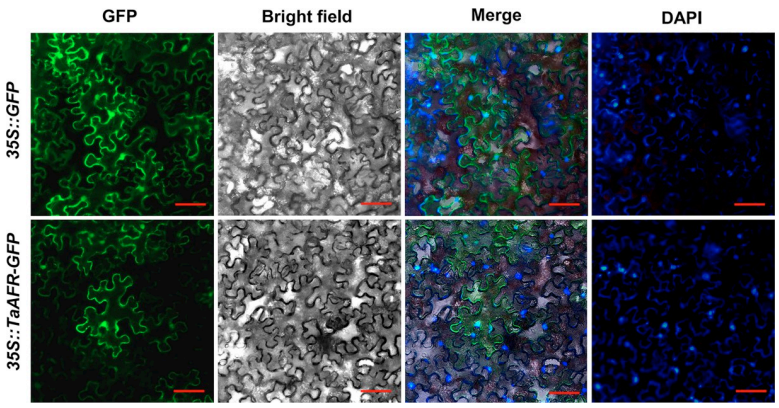

Fig 6. Fluorescence visualization of TaAFR subcellular localization in tobacco leaves. The free GFP protein and TaAFR-GFP fusion protein were transiently expressed in the *N. benthamiana* by *Agtobacterium*-mediated transformation. GFP, GFP fluorescent signal channel; Bright field, ordinary light channel; DAPI, nuclei were stained by DAPI; Merge, merge of GFP, Bright field and DAPI. Bar = 20 μm.

https://doi.org/10.1371/journal.pone.0250479.g006

Screening and identifying TaAFR-interacting proteins

Thirteen putative TaAFR-interactions were identified in a Y2H library screen. To identify candidate upstream and/or downstream proteins interacting with TaAFR in wheat, we screened a yeast library carrying the cDNA of TcLr15 inoculated with the incompatible leaf rust strain against the bait construct, BD-*TaAFR*. Clones from positive interactions were sequenced and thirteen candidate proteins were identified from 47 clones. Candidate proteins are listed in S4 Table, and categorized into the following 5 groups: photosynthesis, stress resistance, transportation, basal metabolism, and unknown protein. Among these, 5 stress resistance related proteins were obtained: peroxidase 51-like (POD), obtusifoliol 14-alpha-demethylase (CYP51), glucan endo-1,3-beta-glucosidase 14 (GV), laccase-7 (Lac7) and leucine-rich repeat protein 1 (LRR-8 superfamily) (LRR) [32–36]. Meanwhile, transport related proteins, ADP-ribosylation factor 2-like isoform X1 (ARL2) and SEC1 family transport protein SLY1 (SLY1), and a basal metabolism related protein, Skp1/ASK1-like protein (Skp1), were also detected [3,37,38].

TaSkp1, TaARL2 and TaPAL interacted with TaAFR. The following 11 genes identified in the Y2H library screen were selected for protein interaction validation: Rubisco, Skp1, ARL2, GV, RP, SLY1, NADH, POD, LRR, Lac7 and CYP51. The complete coding regions were obtained for each of these 11 genes from TcLr15. According to Zhang et al., Kelch repeat F-box proteins are regulated by phenylpropanoid biosynthesis by controlling the turnover of phenylalanine ammonia-lyase (PAL) [11]; therefore, in addition to the positive interactions identified in the Y2H assay, we also isolated a *PAL* gene from TcLr15. Basic characteristics of these 12 proteins are presented in S5 Table. The interactions were first re-verified by Y2H. Colonies with blue pigments are indicative of positive interactions, and along with the positive control, six such interactions were observed: BD-*TaAFR* and AD-*TaSkp1*, BD-*TaAFR* and AD-*TaSLY1*, BD-*TaAFR* and AD-*TaARL2*, BD-*TaAFR* and AD-*TaCYP51*, BD-*TaAFR* and AD-*TaPAL*, BD-*TaAFR* and AD-*TaNADH*. The remaining combinations, along with the negative control, did not grow on the SD-WHLA-X-α-Gal plates. These results suggest that TaAFR may physically interact with TaSkp1, TaSLY1, TaARL2, TaCYP51, TaPAL and TaNADH (Fig 7).

To further validate the above results, these six interactions were tested by BiFC. In this approach, the coding region of the *TaAFR* was inserted downstream of the c-Myc tag of pSPY

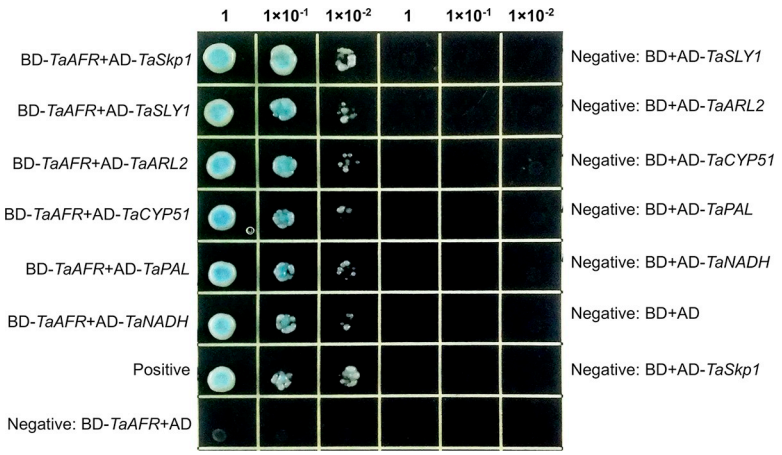

Fig 7. Protein interactions tested by Y2H assay. Yeast was cultivated on SD-WLHA+X-α-Gal plates for 3–5 days.

https://doi.org/10.1371/journal.pone.0250479.g007

CE vector (pSPY CE-*TaAFR*); meanwhile the ORFs of *TaSkp1*, *TaSLY1*, *TaARL2*, *TaCYP51*, *TaPAL* and *TaNADH* were inserted downstream of the 35S promoter in the pSPY NE vector (pSPY NE-*Prey*). The pSPY CE-*TaAFR* vector was used for co-transfection of tobacco leaves with each of the pSPY NE-*Prey* constructs. Among the six combinations, three were found to emit fluorescent signals (Fig 8), indicating that the gene products of those combinations were interacting. pSPY CE-*TaAFR* and pSPY NE-*TaSkp1* emitted a fluorescent signal in the nucleus and cytoplasm 40 h after injection. The pSPY CE-*TaAFR* and pSPY NE-*TaARL2* emitted a strong signal in the nucleus and cytoplasm 48 h after co-transfection. The pSPY CE-*TaAFR* and pSPY NE-*PAL* interaction was observed in the cytoplasm by complementary chimeric fluorescence signals 40 h after co-transfection. Thus, the BiFC assay further validated TaAFR interactions with TaSkp1, TaARL2 and TaPAL.

Co-IP assays were performed to further validate the results tested by Y2H and BiFC *in vivo*. The combinations of TaAFR with three putative partner proteins TaSkp1, TaARL2, TaPAL, and negative control GFP, were successfully detected in the whole cell lysates (WCL) following transient co-expression in *N. benthaminana*. After IP by HA-magnetic beads, the eluted proteins were subjected to immunoblot analysis with anti-FLAG antibody. For each of the HA-purifications, an HC (IgG heavy chain) was detected at 55 kDa. An additional band was detected for each of the three candidate interacting proteins, TaSkp1, TaARL2 and TaPAL, at the expected molecular weights for interaction with TaAFR, indicating that these three proteins were co-immunoprecipitated with TaAFR. By contrast, no additional band was detected in the TaAFR-GFP interaction, as expected for the negative control (Fig 9). It should be noted that a small number of non-specific partial bands were detected in a few cases, but they did not interfere with bands of the interacting protein pairs, nor were they in the expected size range of any of the four proteins of interest. Taken together, these observations support that TaAFR interact with TaSkp1, TaARL2 and TaPAL *in vivo*.

The F-box domain of TaAFR interacted with TaSkp1, and the Kelch domain with TaARL2 and TaPAL. To determine which domain of TaAFR is responsible for recognizing the TaSkp1, TaARL2 and TaPAL, we further obtained the cDNA sequences of the F-box (1–71 aa) and Kelch (72–383 aa) domains of TaAFR, and then constructed recombinant BD vectors for each. Six combinations of AD-*TaSkp1* and BD-*TaAFR-F-box*, AD-*TaSkp1* and BD-*TaAFR-Kelch*, AD-*TaARL2* and BD-*TaAFR-F-box*, AD-*TaARL2* and BD-*TaAFR-Kelch*, AD-*TaPAL* and BD-*TaAFR-F-box*, AD-*TaPAL* and BD-*TaAFR-Kelch* were verified using the Y2H

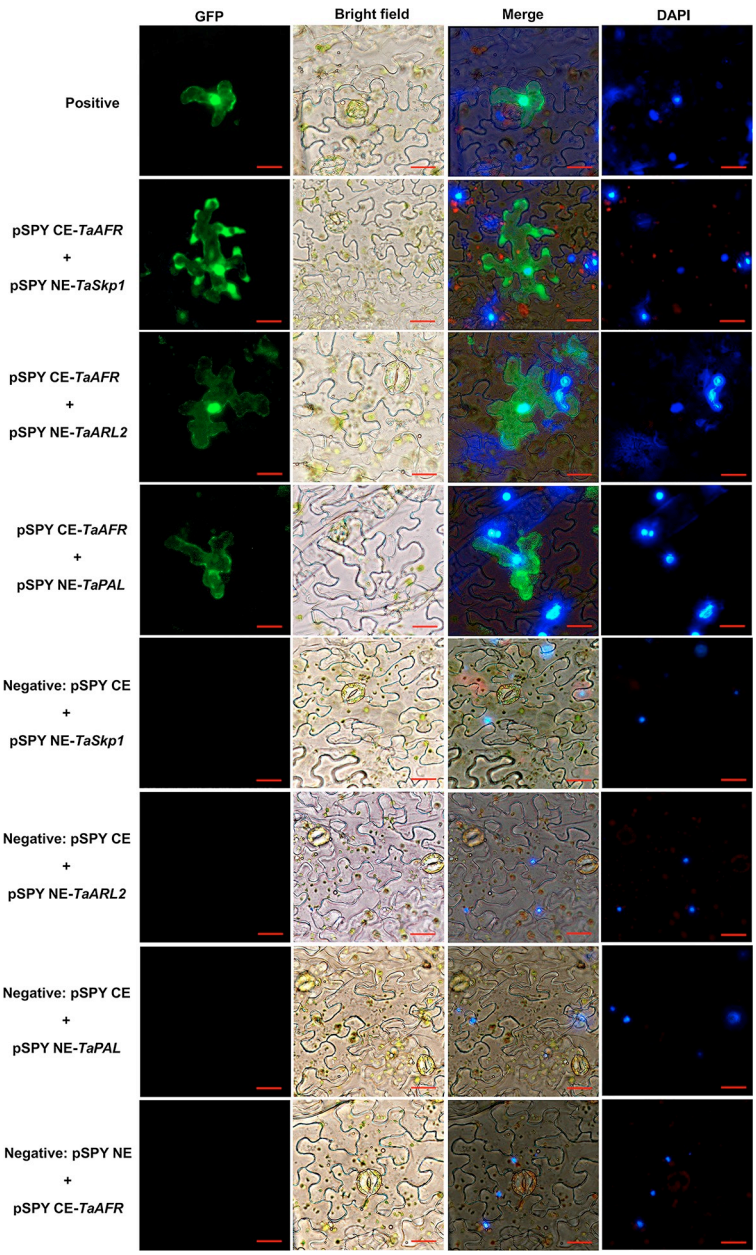

Fig 8. Verification of protein interactions by BiFC assay. The fluorescence microscope (Nikon Ti 2, Japan) with an excitation wavelength of 495 nm was used to observe fluorescence signal. Three independent experiments were conducted for each combination. Bar = 20 μm.

https://doi.org/10.1371/journal.pone.0250479.g008

assay. Among them, three combinations of AD-*TaSkp1* and BD-*TaAFR-F-box*, AD-*TaARL2* and BD-*TaAFR-Kelch*, AD-*TaPAL* and BD-*TaAFR-Kelch* grew well on the SD-WLHA+X-α-Gal plates (Fig 10). These results indicate that TaSkp1 interacted with the F-box domain, while TaARL2 and TaPAL were recognized by the Kelch domain of TaAFR.

Discussion

The Kelch type F-box protein is one of the most common subfamilies of the F-box family proteins in plants [39]. Many wheat databases are being continuously updated, with improved

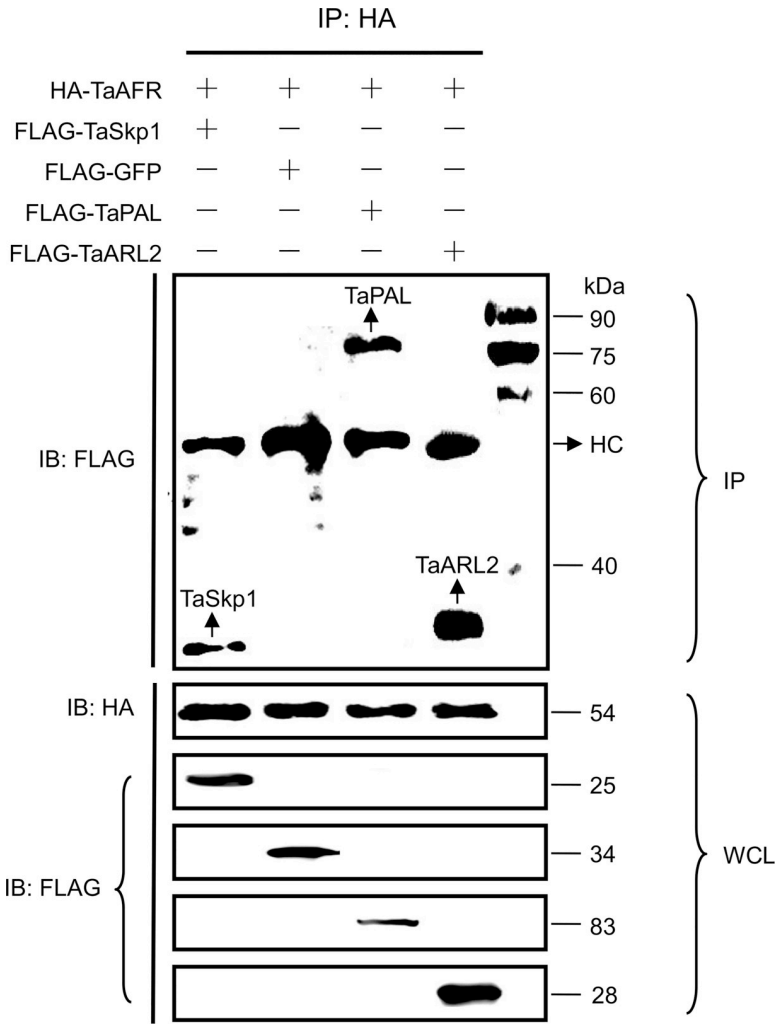

Fig 9. Verification of protein interactions by Co-IP. Proteins were extracted from leaves of *N. benthamiana* 60 h after co-injection, and immunoblotting (IB) was used to detect the expression of TaAFR, TaSkp1, TaARL2, TaPAL and GFP in the WCL with HA or FLAG antibody, these proteins were immunoprecipitated by HA-magnetic beads, then the eluted proteins were subjected to IB analysis with anti-FLAG antibody. HC: IgG heavy chain. Marker: 25–90 kDa.

https://doi.org/10.1371/journal.pone.0250479.g009

annotations over recent years, making it possible for genome-wide identification and comprehensive analysis of gene families. In 2020, Hong et al. reported 41 wheat F-box/Kelch genes [40], and in our previous analysis, 59 wheat F-box/Kelch genes were identified in Phytozome

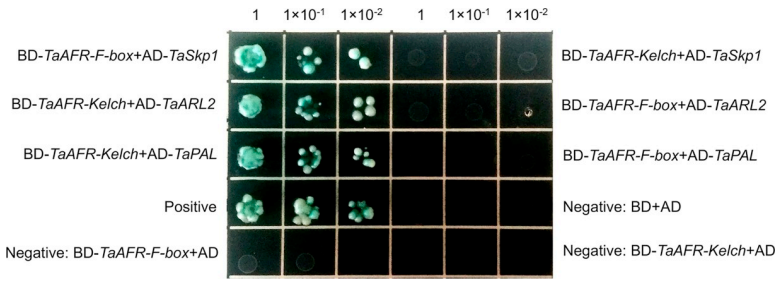

Fig 10. Domain interactions tested by Y2H. Yeast was cultivated on SD-WLHA+X-α-Gal plates for 3–5 days.

https://doi.org/10.1371/journal.pone.0250479.g010

12 (v2.2) [41]. In the present study, we screened IWGSC database in EnsemblPlants with more seed sequences and identified 68 *TaFBK*s encoding 74 putative proteins. The TaFBK subfamily was divided into 7 categories based on differences in the number of Kelch domains present. The majority of the AtFBKs, which showed a relatively distant evolutionary relationship with the four Gramineae species evaluated, resolved to clade G. Meanwhile the TaFBKs resolved into the other six clades (A-F) together with the OsFBKs, SbFBKs and ZmFBKs, and phylogenetic grouping was found to be related to the composition of their functional domains. Compared with the Arabidopsis FBK subfamily, three types of FBKs, namely F-box+4 Kelch, PAC +F-box+4 Kelch and LSM14+F-box+2 Kelch, were not detected in wheat. Each of these types are poorly represented in Arabidopsis, with only one member for each. It may be that they are absent in wheat due to selective evolution of the species, or it may simply be that they cannot yet be detected at the current sequencing depth or annotation of the wheat protein database. F-box+1 Kelch+RING and LSM14+F-box+2 Kelch were found to be unique FBK types in rice and Arabidopsis, respectively.

Studies have shown that FBKs are localized to the nucleus, cytosol and/or organelles. For example, CarF-Box1 (chickpeas) and TML (legume) were found to localize in the nucleus, while TaKFB1 through TaKFB5 (colored wheat) were all co-localized to both the nucleus and cytoplasm [40,42,43]. The wheat FBKs identified herein, were predicted to localize in the nucleus, cytoplasm, plastid and/or other organelles. While these predictions may provide some insights into potential gene function, they are not always accurate. For example, the wheat FBK, TaAFR (TaFBK19), was predicted to localize in the cytosol, but was shown experimentally herein to localize to both the nucleus and the cytoplasm.

To gleam some insights into the potential functionality of the wheat FBKs, their expression was observed in response to different stresses. An initial *in silico* analysis was carried out by comparing the expression of 47 *TaFBKs* in their response to DS, HS, and HD. While the expression patterns varied amongst these genes in response to the different treatments, many of them were strongly down-regulation in response to HS. *TaAFR* was further selected for expression analysis in response to abiotic/biotic stresses and hormone treatments. NaCl and H_2O_2 treatments resulted in the strongest up-regulation of *TaAFR*. Interestingly, *TaAFR* expression patterns showed different trends in response to a virulent *vs* an avirulent strain of the leaf rust pathogen. Many previous studies have reported similar observations for the expression of different plant *FBKs* in response to various abiotic and biotic stresses. For example, the nuclear localized FBK gene *CarF-box1* from chickpea was shown to play an important role in abiotic stress, where expression of this gene was significantly up-regulated after drought and salt treatments, but down-regulated under heat and cold stresses [42]. The grape FBK gene *BIG24.1* was up-regulated by Botrytis infection, and up-regulation of this gene affected the plants response to other biotic and abiotic stresses [44]. In another example, the F-box protein containing two Kelch repeats in sugar beet homologous to Arabidopsis FBK AT1G74510, was found to interact with the beet necrotic yellow vein virus pathogenicity factor P25, and it was speculated that P25 could affect formation of the SCF complex [45].

Biotic and abiotic stress responses are often regulated by plant signaling hormones and exposure to such stresses can activate these pathways [46]. It is therefore interesting that the expression of *TaAFR* was also affected by three different plant hormones. SA, ABA and MeJA treatments had a medium effect on the expression of *TaAFR*, suggesting that this gene may regulate and be regulated by different plant hormones. A regulatory behavior in plant hormone responses would be consistent with the role of FBKs in hormone signaling pathways [22,24].

FBKs interact both with other members of the UPS and with downstream targets for proteasome degradation; identification of some of these interacting proteins can further provide

insight into the function of this protein. A multifaceted approach was employed to identify and validate candidate interactions. First, using a leaf rust pathogen treated TcLr15 wheat leaf cDNA library, a Y2H library screen was utilized as a broad scale approach to fish for candidate interacting proteins. A total of 13 candidates were identified, and 11 of these were cloned and re-screened by Y2H for interactions with TaAFR. Additionally, a *PAL* gene, which was not identified in the pool, but has been shown to be involved in regulation process of FBKs, was added to the list. Among these, a total of 6 interactions, including the TaAFR-TaPAL interaction, were confirmed positives. However, since Y2H assay can pick up false positives, these 6 genes were then validated using the BiFC and Co-IP methods, and finally three partner proteins interacting with TaAFR were confirmed: TaSkp1, TaARL2, and TaPAL.

To further characterize their interactions, another Y2H assay was carried out between the F-box and Kelch domains of TaAFR with each of these proteins. TaSkp1 was shown to interact with the F-box domain but not with the Kelch domain. This was not unexpected since Skp1 is a known component of the SCF complex, and since F-box proteins interact with Skp1 via the F-box domain. This result provides preliminary evidence that TaAFR forms part of the SCF complex. Meanwhile, the other two proteins, TaARL2 and TaPAL, were shown to interact with the Kelch domain, and not the F-box domain, suggesting that these two proteins are targeted by TaAFR for ubiquitination and thus designated for proteolytic degradation.

ARL2 is an ADP ribosylation factor (ARF)-like GTPase and members of the ARF family are known to regulate a wide range of cellular processes in eukaryotes, including mitochondrial fusion and microtubule dynamics [47–49]. Most of what is known about ARL2 proteins comes from research in humans and yeast, with little information in plants. Some plant *ARF* genes have been linked with biotic or abiotic stress responses, either by gene expression analysis [50] or through experimental validation [51]. Guan et al. characterized three *ARF* genes from Switchgrass (*Panicum virgatum* L.), namely *PvArf1*, *PvArf-B1C* and *PvArf-related* [51]. Through transgenic overexpression of these genes, the authors determined that they contribute to salt-tolerance in Switchgrass and that then phenotype was linked to an increase in proline accumulation. They also found that the encoded PvARF proteins interacted with a key enzyme in the proline biosynthesis pathway, PvP5CS1. While the role of TaARL2 in wheat biological processes is yet to be determined, the identification of an interaction between TaARF and TaARL2 through the Kelch domain of TaARF, suggests that this protein might be regulated through the ubiquitination pathway.

PAL activity is modulated by abiotic/biotic stresses in plants, including infections with fungal pathogens, UV/blue light irradiation, and wounding [52]. Zhang et al. found that differential expression of an Arabidopsis *FBK* genes affected the stability of PAL, and PAL isozymes were shown to physically interact with FBKs both *in vitro* and *in vivo* [11]. The interaction of PAL with FBKs thereby controls phenylpropanoid biosynthesis by mediating the ubiquitination and subsequent degradation of PAL. In another study, the authors showed that the Arabidopsis FBK protein, KFB39, a homolog of AtKFB50, also interacted with PAL isozymes and regulated PAL stability and activity, thereby participating in the plant's tolerance to UV irradiation [12]. In the work presented herein, TaAFR interacted with TaPAL, and was shown specifically to interact with the Kelch domain. Based on these results, together with what is known for homologous proteins in Arabidopsis, it is speculated that TaAFR binds Skp1 (through the F-box domain) and the downstream target, TaPAL (through the Kelch domain), forming SCF^{PAL}, thereby regulating PAL stability and activity in the wheat response to abiotic/biotic stresses [11,12].

The detailed protein interacting assays presented indicate that TaAFR is likely to bind TaSkp1, and suggest that TaARL2 and TaPAL are likely downstream targets. Additional studies are needed to determine whether TaAFR is actively involved in the regulation of these

proteins by forming an SCF complex and targeting these proteins for ubiquitination and proteosome degradation. Furthermore, how these putative activities in the regulation of TaARL2 and TaPAL participate in biotic or abiotic stress responses have yet to be investigated. The work presented in this manuscript provides a glimpse into the potential function of TaAFR and their partner proteins, and opens the door for future studies to further characterize these genes.

Conclusion

A total of 68 *TaFBK* genes encoding for 74 proteins were identified in wheat. The FBK proteins from wheat, Arabidopsis and three important monocots were grouped into 7 clades according to the number of Kelch domain. Sixty-eight *TaFBK* genes were unevenly distributed on 21 wheat chromosomes, *TaFBKs* differentially expressed at multiple developmental stages and tissues, and in response to drought and/or heat stresses by *in silico* analysis. A Kelch type F-box gene *TaAFR* was isolated and found to be primarily expressed in wheat leaves, and it's expression was perturbed by various treatments, including exposure to leaf rust pathogens, exogenous plant hormone treatments, and abiotic stresses. The protein was shown to localize in the nucleus and cytoplasm. The wheat Skp1 protein was found to interact with the F-box domain of TaAFR, while ARL2 and PAL were recognized by Kelch domain suggesting that TaAFR targets these two proteins proteasomal degradation. This work provides a foundation from which to build more detailed research inquiries into the function of the numerous wheat FBKs and also to further characterize the *TaAFR* gene.

Supporting information

S1 Fig. Classification of FBK proteins in wheat based on different functional domains. F-box, the protein with F-box domain; Kelch, F-box protein having Kelch domain; PAS, FBK protein with PAS domain that was named after three proteins that it occurs in: Per-period circadian protein, Arnt-Ah receptor nuclear translocator protein and Sim-single-minded protein; PAC, FBK protein with PAC domain that usually appears at the C-terminus of the PAS motif.
(TIF)

S2 Fig. WebLogo generated by alignments of the F-box (A) or Kelch (B) domains of wheat FBKs. The F-box or Kelch motifs were retrieved from 74 wheat F-box proteins. The overall height of every stack is indicative of sequence conservation at the given position within the motif, whereas the height of the letters within each stack is indicative of the relative frequency of the corresponding amino acid. The bit score represents the information content for each position. Asterisks mark the conserved residues.
(TIF)

S3 Fig. Chromosomal distribution of wheat *FBK* genes. The chromosomes were drafted to proportion and the chromosome numbers were indicated at the top of each stave. Chromosomal distances were given in megabases (10 Mb). The gene names were listed at the right side of each chromosome corresponding to the position of each gene. Tandemly duplicated genes were shown in pink boxes. Segmental duplications were shown in colored blocks.
(TIF)

S1 Table. Primer sequences.
(DOC)

S2 Table. Characteristics of wheat, Arabidopsis, rice, sorghum and maize FBK proteins.
(XLS)

S3 Table. FPKM values of wheat *FBK* genes.
(XLS)

S4 Table. Screening of the candidate proteins interacting with TaAFR.
(DOC)

S5 Table. Bioinformatics analysis of the candidate proteins.
(DOC)

S1 File. Sequences of FBK proteins in wheat, Arabidopsis, rice, sorghum and maize.
(FASTA)

S1 Raw images.
(PDF)

Author Contributions

Conceptualization: Chunru Wei, Xiumei Yu.

Data curation: Chunru Wei, Runqiao Fan.

Funding acquisition: Xiumei Yu.

Investigation: Chunru Wei, Yuyu Meng.

Methodology: Yiming Yang, Xiaodong Wang.

Project administration: Xiumei Yu.

Software: Chunru Wei.

Writing – original draft: Chunru Wei.

Writing – review & editing: Weiquan Zhao, Nora A. Foroud, Daqun Liu, Xiumei Yu.

References

1. Nguyen KM, Busino L. The biology of F-box proteins: The SCF family of E3 ubiquitin ligases. Adv Exp Med Biol. 2020; 1217: 111–122. https://doi.org/10.1007/978-981-15-1025-0_8 PMID: 31898225
2. Au W, Zhang T, Mishra P K, Eisenstatt JR, Walker RL, Ocampo J, et al. Skp, Cullin, F-box (SCF)-Met30 and SCF-Cdc4-mediated proteolysis of CENP-A prevents mislocalization of CENP-A for chromosomal stability in budding yeast. PLoS Genet. 2020; 16: e1008597. https://doi.org/10.1371/journal.pgen.1008597 PMID: 32032354
3. HajSalah El Beji I, Mouzeyar S, Bouzidi MF, Roche J. Expansion and functional diversification of *SKP1-like* genes in wheat (*Triticum aestivum* L.). Int J Mol Sci. 2019; 20: 3295–3312. https://doi.org/10.3390/ijms20133295 PMID: 31277523
4. Jain MK, Nijhawan A, Arora R, Agarwal A, Ray S, Sharma P, et al. F-box proteins in rice. Genome-wide analysis, classification, temporal and spatial gene expression during panicle and seed development, and regulation by light and abiotic stress. Plant Physiol. 2007; 143: 1467–1483. https://doi.org/10.1104/pp.106.091900 PMID: 17293439
5. Xue F, Cooley L. Kelch encodes a component of intercellular bridges in *Drosophila* egg chambers. Cell. 1993; 72: 681–693. https://doi.org/10.1016/0092-8674(93)90397-9 PMID: 8453663
6. Xu G, Ma H, Nei M, Kong HZ. Evolution of F-box genes in plants: Different modes of sequence divergence and their relationships with functional diversification. Proc Natl Acad Sci USA. 2009; 106: 835–840. https://doi.org/10.1073/pnas.0812043106 PMID: 19126682
7. Schumann N, Navarroquezada A, Ullrich KK, Kuhl C, Quint M. Molecular evolution and selection patterns of plant F-box proteins with C-terminal Kelch repeats. Plant Physiol. 2011; 155: 835–850. https://doi.org/10.1104/pp.110.166579 PMID: 21119043
8. Imaizumi T, Schultz TF, Harmon FG, Ho LA, Kay SA. FKF1 F-box protein mediates cyclic degradation of a repressor of CONSTANS in Arabidopsis. Science. 2005; 309: 293–297. https://doi.org/10.1126/science.1110586 PMID: 16002617

9. Shao T, Qian Q, Tang D, Chen J, Li M, Cheng ZK, et al. A novel gene *IBF1* is required for the inhibition of brown pigment deposition in rice hull furrows. Theor Appl Genet. 2012; 125: 381–390. https://doi.org/10.1007/s00122-012-1840-8 PMID: 22419106

10. Curtis RHC, Powers SJ, Napier J, Napier JA, Matthes MC. The Arabidopsis F-box/Kelch-repeat protein At2g44130 is upregulated in giant cells and promotes nematode susceptibility. Mol Plant Microbe Interact. 2013; 26: 36–43. https://doi.org/10.1094/MPMI-05-12-0135-FI PMID: 23075039

11. Zhang X, Gou M, Liu CJ. Arabidopsis Kelch repeat F-box proteins regulate phenylpropanoid biosynthesis via controlling the turnover of phenylalanine ammonia-lyase. Plant Cell. 2013; 25: 4994–5010. https://doi.org/10.1105/tpc.113.119644 PMID: 24363316

12. Zhang X, Gou M, Guo C, Yang HJ, Liu CJ. Down-regulation of Kelch domain-containing F-box protein in Arabidopsis enhances the production of (poly) phenols and tolerance to ultraviolet radiation. Plant Physiol. 2015; 167: 337–350. https://doi.org/10.1104/pp.114.249136 PMID: 25502410

13. Appels R, Eversole K, Stein N, Feuillet C, Keller B, Rogers J, et al. Shifting the limits in wheat research and breeding using a fully annotated reference genome. Science. 2018; 361: e7191. https://doi.org/10.1126/science.aar7191 PMID: 30115783

14. Jia FJ, Wu BJ, Li H, Huang JG, Zheng CC. Genome-wide identification and characterisation of F-box family in maize. Mol Genet Genomics. 2013; 288: 559–577. https://doi.org/10.1007/s00438-013-0769-1 PMID: 23928825

15. Liu R, Meng J. MapDraw: a microsoft excel macro for drawing genetic linkage maps based on given genetic linkage data. Hereditas. 2003; 25: 317–321. https://doi.org/10.3321/j.issn:0253–9772.2003.03.019 PMID: 15639879

16. Hou XJ, Li SB, Liu SR, Hu CG, Zhang JZ. Genome-wide classification and evolutionary and expression analyses of citrus MYB transcription factor families in sweet orange. PLoS ONE. 2014; 9: e11237542. https://doi.org/10.1371/journal.pone.0112375 PMID: 25375352

17. Cannon SB, Mitra A, Baumgarten A, Young ND, May G. The roles of segmental and tandem gene duplication in the evolution of large gene families in *Arabidopsis thaliana*. BMC Plant Biol. 2004; 4: 10–10. https://doi.org/10.1186/1471-2229-4-10 PMID: 15171794

18. Choulet F, Alberti A, Theil A, Glover N, Barbe V, Daron J, et al. Structural and functional partitioning of bread wheat chromosome 3B. Science. 2014; 345: e124972143. https://doi.org/10.1126/science.1249721 PMID: 25035497

19. Liu Z, Xin M, Qin J, Peng H, Ni Z, Yao Y, et al. Temporal transcriptome profiling reveals expression partitioning of homeologous genes contributing to heat and drought acclimation in wheat (*Triticum aestivum* L.). BMC Plant Biol. 2015; 15:152. https://doi.org/10.1186/s12870-015-0511-8 PMID: 26092253

20. Yu X, Zhao W, Yang W, Liu F, Chen J, Goyer C, et al. Characterization of a hypersensitive response-induced gene *TaHIR3* from wheat leaves infected with leaf rust. Plant Mol Biol Rep. 2013; 31: 314–322. https://doi.org/10.1007/s11105-012-0504-9

21. Li FT, Chen XL, Liu CG, Sun Y, Ma H, Zhang T, et al. Effects of different nutrient solutions on growth and ornamental quality of hydroponic *Hyacinthus orientalis* L. Journal of Central South University of Forestry & Technology. 2012; 32: 130–134. https://doi.org/10.14067/j.cnki.1673-923x.2012.10.021

22. Hong MJ, Kim DY, Kang SY, Kim DS, Kim JB, Seo YW. Wheat F-box protein recruits proteins and regulates their abundance during wheat spike development. Mol Biol Rep. 2012; 39: 9681–9696. https://doi.org/10.1007/s11033-012-1833-3 PMID: 22729884

23. Cao Y, Ji HT, Pei XX, Zheng J, Wang M, Ma XF, et al. Evaluation of drought resistance of six winter wheat seeds under PEG simulated drought stress. Journal of Shanxi Agricultural Sciences. 2016; 44: 723–725.

24. Kim YY, Cui MH, Noh MS, Jung KW, Shin JS. The FBA motif-containing protein AFBA1 acts as a novel positive regulator of ABA response in Arabidopsis. Plant Cell Physiol. 2017; 58: 574–586. https://doi.org/10.1093/pcp/pcx003 PMID: 28184867

25. An C, Mou Z. Salicylic acid and its function in plant immunity. J Integr Plant Biol. 2011; 53: 412–428. https://doi.org/10.1111/j.1744-7909.2011.01043.x PMID: 21535470

26. Lim J, Lim CW, Lee SC. Functional analysis of pepper F-box protein CaDIF1 and its interacting partner CaDIS1: Modulation of ABA signalling and drought stress response. Front Plant Sci. 2019; 10: e01365. https://doi.org/10.3389/fpls.2019.01365 PMID: 31737002

27. Wei CR, Fan RQ, Meng YY, Yang YM, Wang XD, Laroche A, et al. Molecular identification and acquisition of interacting partners of a novel wheat F-box/Kelch gene *TaFBK*. Physiol Mol Plant P. 2020; 112: e101564. https://doi.org/10.1016/j.pmpp.2020.101564

28. Ma N, Qiao JZ, Tang WQ, Sun TJ, Liu Nan, Chen Y, et al. Interaction between wheat translationally controlled tumor protein TCTP and SNF1-related protein kinase SnRK1. Chinese Journal of Biotechnology. 2019; 35: 1686–1697. https://doi.org/10.13345/j.cjb.190055 PMID: 31559750

29. Zhu L, Huq E. Characterization of light-regulated protein-protein interactions by in vivo coimmunoprecipitation (Co-IP) assays in plants. Methods Mol Biol. 2019; 2026: 29–39. https://doi.org/10.1007/978-1-4939-9612-4_3 PMID: 31317401

30. Koralewski TE, Krutovsky KV. Evolution of exon-intron structure and alternative splicing. PLoS ONE. 2011; 6: e18055. https://doi.org/10.1371/journal.pone.0018055 PMID: 21464961

31. Jin J, Cardozo T, Lovering RC, Elledge SJ, Pagano M, Harper JW. Systematic analysis and nomenclature of mammalian F-box proteins. Genes Dev. 2004; 18: 2573–2580. https://doi.org/10.1101/gad.1255304 PMID: 15520277

32. Beffa RS, Neuhaus JM, Meins F. Physiological compensation in antisense transformants: specific induction of an "ersatz" glucan endo-1,3-beta-glucosidase in plants infected with necrotizing viruses. Proc Natl Acad Sci USA. 1993; 90: 8792–879616. https://doi.org/10.1073/pnas.90.19.8792 PMID: 8415609

33. Hong SH, Lee SS, Chung JM, Jung HS, Singh S, Mondal S, et al. Site-specific mutagenesis of yeast 2-Cys peroxiredoxin improves heat or oxidative stress tolerance by enhancing its chaperone or peroxidase function. Protoplasma. 2017; 254: 327–334. https://doi.org/10.1007/s00709-016-0948-0 PMID: 26843371

34. Wang Q, Li G, Zheng K, Zhu X, Ma J, Wang D, et al. The soybean *Laccase* gene family: Evolution and possible roles in plant defense and stem strength selection. Genes. 2019; 10: 9. https://doi.org/10.3390/genes10090701 PMID: 31514462

35. Bianchet C, Wong A, Quaglia M, Alqurashi M, Gehring C, Ntoukakis V, et al. An Arabidopsis thaliana leucine-rich repeat protein harbors an adenylyl cyclase catalytic center and affects responses to pathogens. J Plant Physiol. 2019; 232: 12–22. https://doi.org/10.1016/j.jplph.2018.10.025 PMID: 30530199

36. Binjubair FA, Parker JE, Warrilow AG, Puri K, Braidley PJ, Tatar E, et al. Small-molecule inhibitors targeting sterol 14α-demethylase (CYP51): Synthesis, molecular modelling and evaluation against *Candida albicans*. ChemMedChem. 2020; 15: 1294–1309. https://doi.org/10.1002/cmdc.202000250 PMID: 32459374

37. McElver J, Patton D, Rumbaugh M, Liu CM, Yang LJ, Meinke DW. The *TITAN5* gene of Arabidopsis encodes a protein related to the ADP ribosylation factor family of GTP binding proteins. Plant Cell. 2000; 12: 1379–1392. https://doi.org/10.1105/tpc.12.8.1379 PMID: 10948257

38. Toonen Ruud FG, Verhage M. Vesicle trafficking: pleasure and pain from *SM* genes. Trends Cell Biol. 2003; 13: 177–186. https://doi.org/10.1016/s0962-8924(03)00031-x PMID: 12667755

39. Hassan MN, Zainal Z, Ismail I. Plant Kelch containing F-box proteins: structure, evolution and functions. RSC Adv. 2015; 5: 42808–42814. https://doi.org/10.1039/C5RA01875G

40. Hong MJ, Kim DY, Choi H, Seo YW, Kim J. Isolation and characterization of Kelch repeat-containing F-box proteins from colored wheat. Mol Biol Rep. 2020; 47: 1129–1141. https://doi.org/10.1007/s11033-019-05210-x PMID: 31907740

41. Li HY, Wei CR, Meng YY, Fan RQ, Zhao WQ, Wang XD, et al. Identification and expression analysis of some wheat F-box subfamilies during plant development and infection by *Puccinia triticina*. Plant Physiol Bioch. 2020; 155: 535–548. https://doi.org/10.1016/j.plaphy.2020.06.040 PMID: 32836199

42. Jia Y, Gu H, Wang X, Chen QJ, Shi SB, Zhang JS, et al. Molecular cloning and characterization of an F-box family gene *CarF-box1* from chickpea (*Cicer arietinum* L.). Mol Biol Rep. 2012; 39: 2337–2345. https://doi.org/10.1007/s11033-011-0984-y PMID: 21667242

43. Takahara M, Magori S, Soyano T, Okamoto S, Yoshida C, Yano C, et al. TOO MUCH LOVE, a novel Kelch repeat-containing F-box protein, functions in the long-distance regulation of the legume-rhizobium symbiosis. Plant Cell Physiol. 2013; 54: 433–447. https://doi.org/10.1093/pcp/pct022 PMID: 23390201

44. Paquis S, Mazeyratgourbeyre F, Fernandez O, Crouzet J, Clement C, Baillieul F, et al. Characterization of a F-box gene up-regulated by phytohormones and upon biotic and abiotic stresses in grapevine. Mol Biol Rep. 2011; 38: 3327–3337. https://doi.org/10.1007/s11033-010-0438-y PMID: 21104020

45. Thiel H, Hleibieh K, Gilmer D, Varrelmann M. The P25 pathogenicity factor of Beet necrotic yellow vein virus targets the sugar beet 26S proteasome involved in the induction of a hypersensitive resistance response via interaction with an F-box protein. Mol Plant Microbe In. 2012; 25: 1058–1072. https://doi.org/10.1094/MPMI-03-12-0057-R PMID: 22512382

46. Ullah F, Xu Q, Zhao Y, Zhou DX. Histone deacetylase HDA710 controls salt tolerance by regulating ABA signaling in rice. J Integr Plant Biol. 2021; 63: 451–467. https://doi.org/10.1111/jipb.13042 Epub ahead of print. PMID: 33289304.

47. Wätzlich D, Vetter I, Gotthardt K, Miertzschke M, Chen YX, Wittinghofer A, et al. The interplay between RPGR, PDEδ and Arl2/3 regulate the ciliary targeting of farnesylated cargo. EMBO Rep. 2013; 14: 465–472. https://doi.org/10.1038/embor.2013.37 PMID: 23559067

48. Schiavon CR, Turn RE, Newman LE, Kahn RA. ELMOD2 regulates mitochondrial fusion in a mitofusin-dependent manner, downstream of ARL2. Mol Biol Cell. 2019; 30: 1198–1213. https://doi.org/10.1091/mbc.E18-12-0804 PMID: 30865555

49. Zhou C, Cunningham L, Marcus AI, Li Y, Kahn RA. Arl2 and Arl3 regulate different microtubule-dependent processes. Mol Biol Cell. 2006; 17: 2476–2487. https://doi.org/10.1091/mbc.e05-10-0929 PMID: 16525022

50. Li YQ, Song JH, Zhu G, Hou ZH, Wang L, Wu XX, et al. Genome-wide identification and expression analysis of ADP-ribosylation factors associated with biotic and abiotic stress in wheat (*Triticum aestivum* L.). PeerJ. 2021; 9: e10963. https://doi.org/10.7717/peerj.10963 PMID: 33717696

51. Guan C, Li X, Tian DY, Liu HY, Cen HF, Tadege M, et al. ADP-ribosylation factors improve biomass yield and salinity tolerance in transgenic switchgrass (*Panicum virgatum* L.). Plant Cell Rep. 2020; 39: 1623–1638. https://doi.org/10.1007/s00299-020-02589-x PMID: 32885306

52. Dixon RA, Paiva NL. Stress-induced phenylpropanoid metabolism. Plant Cell. 1995; 7: 1085–1097. https://doi.org/10.1105/tpc.7.7.1085 PMID: 12242399